Materials Science-Poland, Vol. 23, No. 2, 2005

Molecular dynamics of cholesterol in a thin film surrounding a carbon nanotube

PRZEMYSŁAW RACZYŃSKI*, ALEKSANDER DAWID, MARIUSZ SOKÓŁ, ZYGMUNT GBURSKI

Institute of Physics, University of Silesia, Uniwersytecka 4, 40-007 Katowice, Poland

Molecular dynamics (MD) simulations of the system composed of a single walled carbon nanotube (SWNT) surrounded by a thin film of: a) cholesterol–water mixture and b) pure cholesterol have been carried out. The translational and rotational correlation functions and their Fourier transforms of both cholesterol and water molecules have been calculated for several temperatures and concentrations. The interpretation of translational and rotational dynamics of both cholesterol and water molecules in the specific environment is presented.

Key words: *single walled carbon nanotube; MD simulation; thin film; cholesterol; water*

1. Introduction

The discovery of carbon nanotubes [1] has initiated a number of scientific investigations devoted to the study of their mechanical, chemical, optical, thermal and electrical properties [2–6]. Recently, however, there has been increasing activity in investigating small, finite size SWNT-based mixture systems, because they are expected to exhibit interesting properties for nanotechnological applications [7, 8]. This paper presents a classical molecular dynamics simulation (MD) [9] study of the single-walled carbon nanotube surrounded by cholesterol molecules and a cholesterol–water mixture.

2. Simulation details

As a typical representative of the family of carbon nanotubes an armchair (10, 10) nanotube [7] was chosen. The Lennard–Jones (L–J) interaction potential V between

* Corresponding author, e-mail: praczyns@us.edu.pl

the carbon atoms of the nanotube and the sites (atoms) of the cholesterol molecule (Fig. 1) as well as between cholesterol sites was applied.

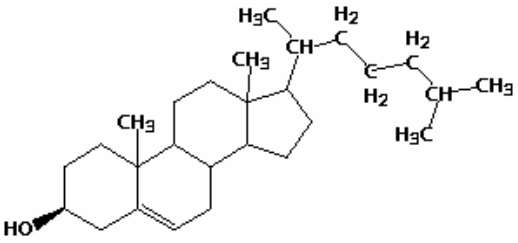

Fig. 1. The structure of the cholesterol molecule

The L–J potential energy is given by the formula:

$$V(r_{ij}) = 4\varepsilon\left[\left(\frac{\sigma}{r_{ij}}\right)^{12} - \left(\frac{\sigma}{r_{ij}}\right)^{6}\right] \tag{1}$$

where ε is the minimum of the potential at a distance of $2^{1/6}\sigma$, k_B is the Boltzmann constant and r_{ij} is the distance between the atoms i and j. The parameters used in Eq. (1) are given in Table 1 [10].

Table 1. Lennard–Jones potential parameters

Atoms	ε/k_B [K]	σ [Å]	m [10^{-25} kg]
C	58.2	3.851	0.199
O	88.7	2.95	0.26551
H	12.4	2.81	0.016594

The L–J potential parameters between unlike atoms are given by the Lorentz –Berthelot rules [9] $\sigma_{A-B} = (\sigma_A + \sigma_B)/2$ and $\varepsilon_{A-B} = \sqrt{\varepsilon_A \varepsilon_B}$, where A, B are C, O or H atoms. We applied an approach involving the TIP4P model of the water molecule [11, 12], which provides a reasonable description of liquid water and aqueous solutions [11]. This model is based on four interaction sites located in a planar configuration, two of which (H) are associated with protons and another two (M and O) are associated with the oxygen nucleus. The angle between H, O and another H site is $\sphericalangle$ HOH = 104°52′. The distances between O and H, and between the O and M sites are r_{OM} = 0.15 Å and r_{OH} = 0.9572 Å, respectively. The interactions between the molecules are described in terms of the pairwise potential composed of the Lennard–Jones and Coulombic components:

$$V_{\text{wat.}}(r_{ij}) = \sum_{m\in i}\sum_{n\in j}\frac{q_m q_n e^2}{r_{im,jn}} + \frac{A}{r_{OO}^{12}} - \frac{B}{r_{OO}^{6}} \tag{2}$$

where r_{OO} is the distance between the i-th and j-th oxygen atoms and $r_{im,jn}$ are the distances between all pairs of charges. The charges appearing in the potential are $q_H = 0.52e$, $q_M = -1.04e$ and $q_O = 0$, where $e^2 = 331.8$ (kcal·Å)/mol. As a part of the molecular design process, the negative charge has been shifted away from the O site by a small amount to the M site, which has been introduced specifically for this purpose. The rest of the parameters appearing in the L–J-part of Eq. (2), which acts only between the O sites, are $A = 600.0\times10^3$ (kcal·Å^{12})/mol and $B = 610.0$ (kcal·Å^6)/mol.

The classical equations of motion are integrated up to 5 ns by the predictor –corrector Adams–Moulton algorithm [13]. The integration time step was 0.4 fs which ensures total energy conservation within 0.01 %. The initial positions were generated by the Monte Carlo method [9] and initially equilibrated over 10^6 MD time steps before the MD data were calculated and collated.

3. Results

Firstly one single armchair carbon nanotube surrounded by a varying number n = 3, 5, 9 of cholesterol molecules was simulated, for several temperatures. In Fig. 2 the calculated mean square displacement $\left\langle \left|\Delta\vec{r}\,(t)\right|^2 \right\rangle$ of the centre of mass of cholesterol is presented, where

$$\left\langle \left|\Delta\vec{r}\,(t)\right|^2 \right\rangle = \left\langle \left|\vec{r}\,(t) - \vec{r}\,(0)\right|^2 \right\rangle$$

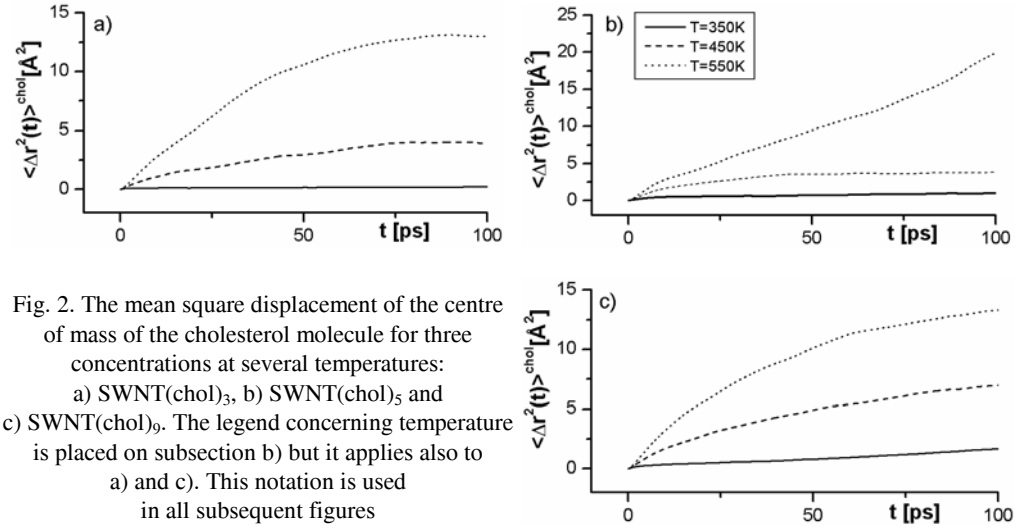

Fig. 2. The mean square displacement of the centre of mass of the cholesterol molecule for three concentrations at several temperatures: a) SWNT(chol)$_3$, b) SWNT(chol)$_5$ and c) SWNT(chol)$_9$. The legend concerning temperature is placed on subsection b) but it applies also to a) and c). This notation is used in all subsequent figures

and $\vec{r}$ is the position of the centre of mass of a single molecule [14]. The mean square displacement is connected with the diffusion coefficient *via* Einstein relation

$$\left\langle \left| \Delta \vec{r}\,(t) \right|^2 \right\rangle \approx 6Dt$$

where D is the translational diffusion coefficient.

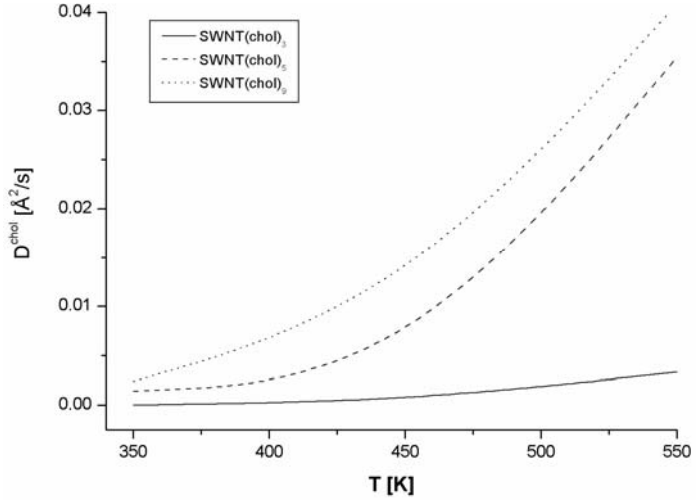

Fig. 3. The translational diffusion coefficient D of the centre of mass of the cholesterol molecule for three concentrations as a function of temperature

It can be seen in Figures 2 and 3 that at low temperature, T = 350 K, a solid phase appears (no diffusion, $D \approx 0$), whereas the fluid phase is observed at higher temperatures. The distinction between solid (T = 350 K) and liquid (T = 550 K) phase can be also seen in Fig. 4, where an example of the radial distribution function $g(r)$ [9] of the centre of mass of cholesterol (n = 9) is given.

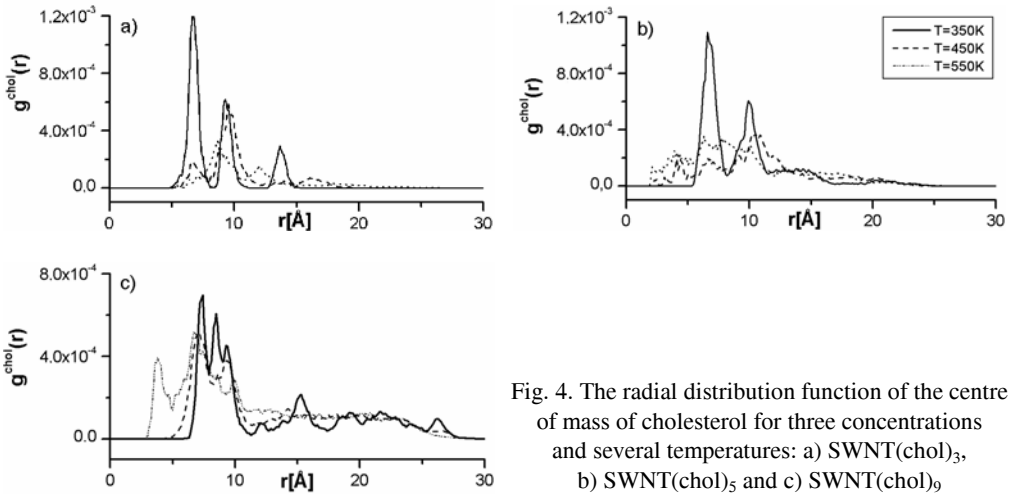

Fig. 4. The radial distribution function of the centre of mass of cholesterol for three concentrations and several temperatures: a) SWNT(chol)$_3$, b) SWNT(chol)$_5$ and c) SWNT(chol)$_9$

Note that the translational mobility of cholesterol's fluid phase in the layer which covers the SWNT increases with a growing number n of cholesterol molecules. In the case of small n each particular molecule is in direct contact with the SWNT's surface being strongly attracted by the carbon atoms of the nanotube. More cholesterol molecules (larger n) means more interactions between the cholesterol sites, the tight binding of cholesterol molecules to the nanotube's surface is partially weakened by non-negligible cholesterol–cholesterol interactions and the increased ability of the cholesterol molecules to move over the nanotube's surface. A representative snapshot of the fluid state configuration of the system studied ($n = 9$) is presented in Fig. 5.

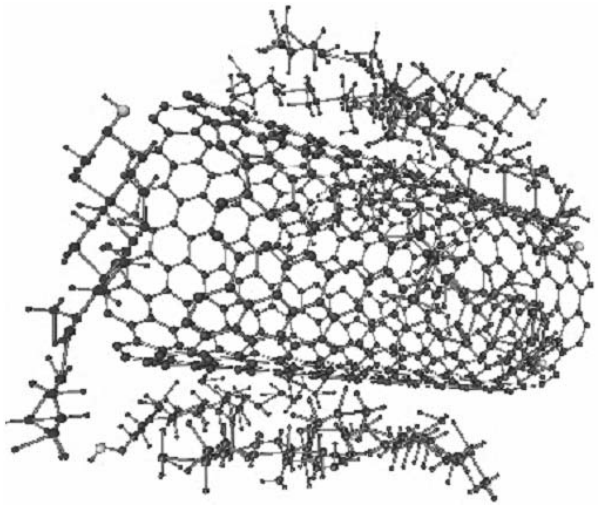

Fig. 5. An example of the liquid state instantaneous configuration of the SWNT(chol)$_9$ cluster at T=550 K

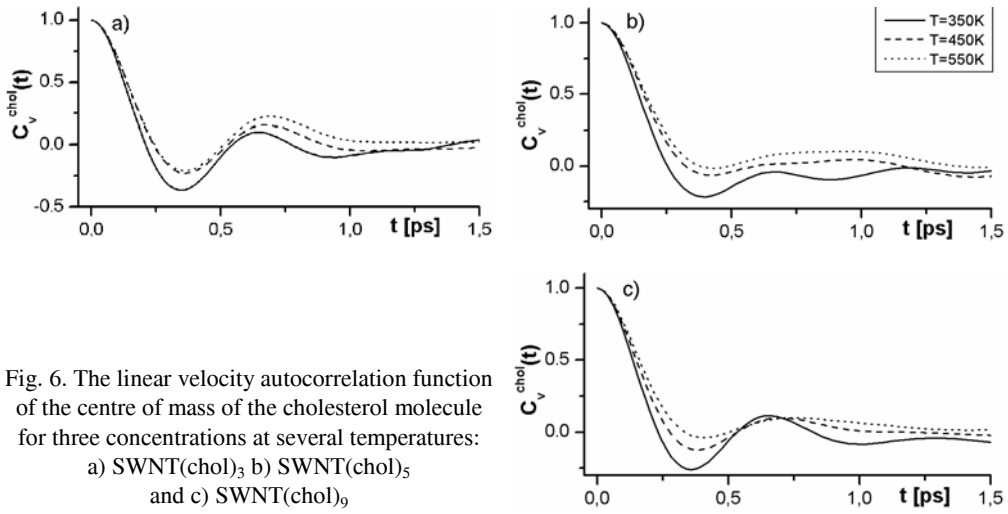

Fig. 6. The linear velocity autocorrelation function of the centre of mass of the cholesterol molecule for three concentrations at several temperatures: a) SWNT(chol)$_3$ b) SWNT(chol)$_5$ and c) SWNT(chol)$_9$

Closely connected with the translational motion is the velocity autocorrelation function $C_{\vec{v}}(t) = \langle \vec{v}(t)\vec{v}(0) \rangle \langle \vec{v}(0)\vec{v}(0) \rangle^{-1}$, where $\vec{v}(t)$ is the translational velocity of the molecule. The behaviour of the calculated correlation functions $C_v(t)$ of cholesterol can be seen in Fig. 6.

The strong oscillations of $C_v(t)$ at low temperatures – characteristic of the solid state [9] – become gradually smoother and less pronounced at higher temperatures as a result of significant randomization of $\vec{v}(t)$ in the liquid phase. Examples of the corresponding Fourier transforms

$$FT(C_{\vec{v}}(t)) = \int_0^\infty C_{\vec{v}}(t)\cos(2\pi\nu t)\,dt$$

are given in Fig. 7.

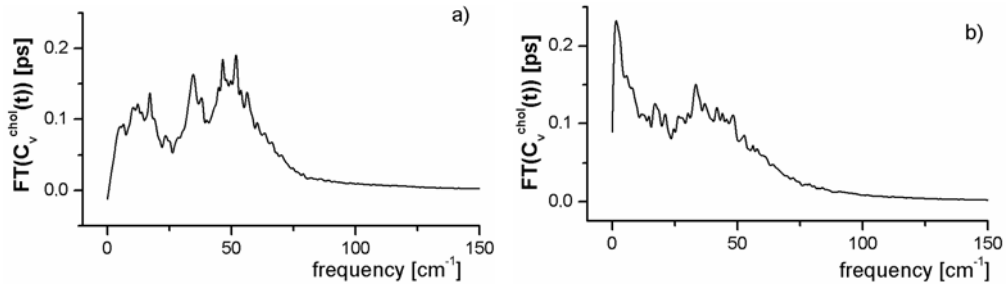

Fig. 7. The Fourier transform $FT(C_{\vec{v}}(t))$ of the linear velocity correlation function of the cholesterol for the solid a) and liquid b) phase of SWNT(chol)$_9$

Two characteristic modulation frequencies are clearly visible at low temperature. The lower frequency ($\nu \approx 20$ cm^{-1}) is associated with the back and forth pulling of cholesterol by the nanotube and the higher frequency ($\nu \approx 50$ cm^{-1}) is connected with cholesterol librations within the layer of cholesterol molecules composed around the nanotube. The higher frequency peak becomes broader and less defined as a result of mutual and random collisions of cholesterol molecules in the liquid state.

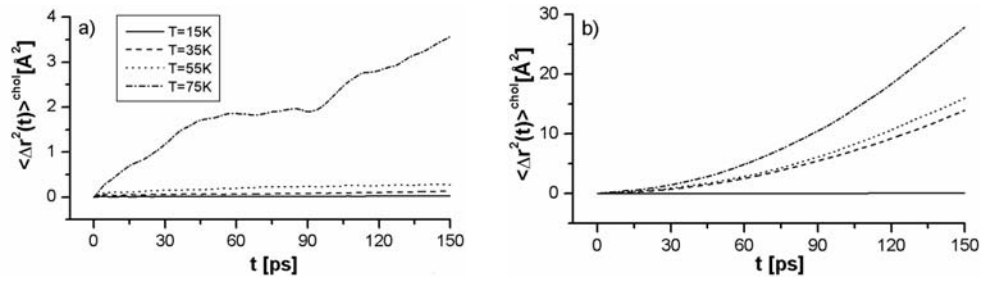

Fig. 8. The mean square displacement of the centre of mass of the cholesterol molecule for two concentrations at several temperatures: a) SWNT(chol)$_3$(water)$_{45}$ and b) SWNT(chol)$_2$(water)$_{80}$

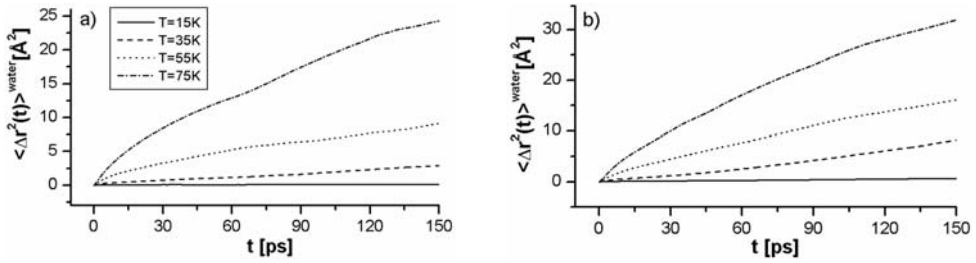

Fig. 9. The mean square displacement of the centre of mass of the water molecule for two concentrations at several temperatures: a) SWNT(chol)$_3$(water)$_{45}$ and b) SWNT(chol)$_2$(water)$_{80}$

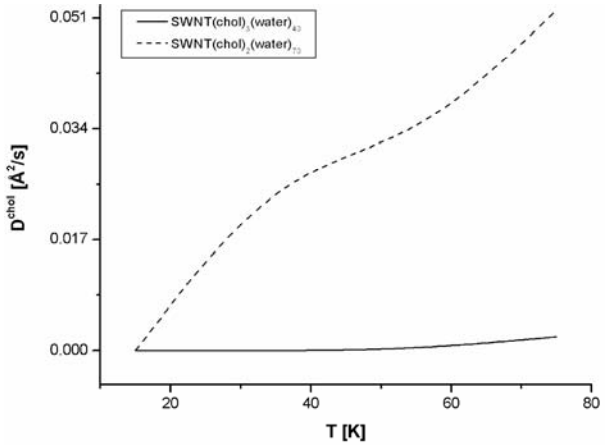

Fig. 10. The translational diffusion coefficient of the centre of mass of the cholesterol molecule for two concentrations as a function of temperature

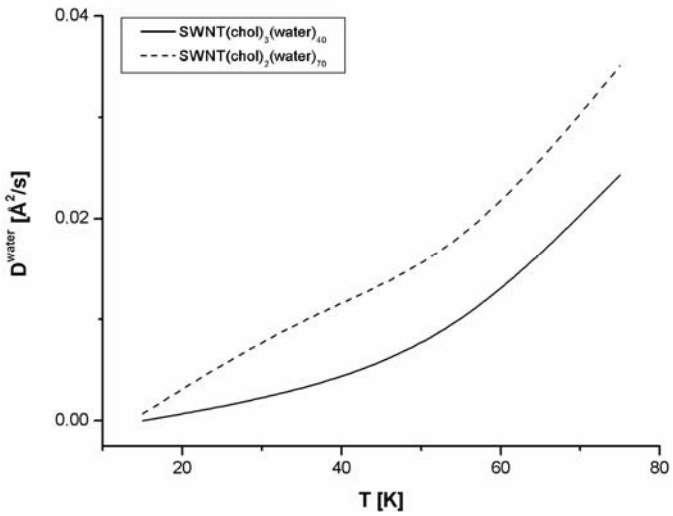

Fig. 11. The translational diffusion coefficient of the centre of mass of the water or two concentrations as a function of temperature

The second part of the work focussed on the properties of a cholesterol–water mixture surrounded an armchair (10, 10) single walled carbon nanotube. The motivation was, that in living cells, cholesterol usually appears accompanied by water. Two concentrations of the cholesterol–water mixture: $SWNT(chol)_3(water)_{45}$ and $SWNT(chol)_2(water)_{80}$ were studied. The mean square displacement of the centre of mass of both, cholesterol and water molecules, is shown in Figs. 8 and 9, respectively.

The liquid phase developed here at much lower temperature, comparing to the previous system (pure cholesterol layer). The diffusion coefficients of cholesterol and water molecules are presented in Fig 10 and Fig 11.

The presence of water molecules significantly changes the dynamics of the cholesterol molecules. Note the substantial increase of the value of D_{chol} for the cholesterol–water mixture compared to the cholesterol only layer. An example of the simulated radial distribution functions of the centre of mass of cholesterol and water molecules $SWNT(chol)_2(water)_{80}$ is given in Figs. 12 and 13.

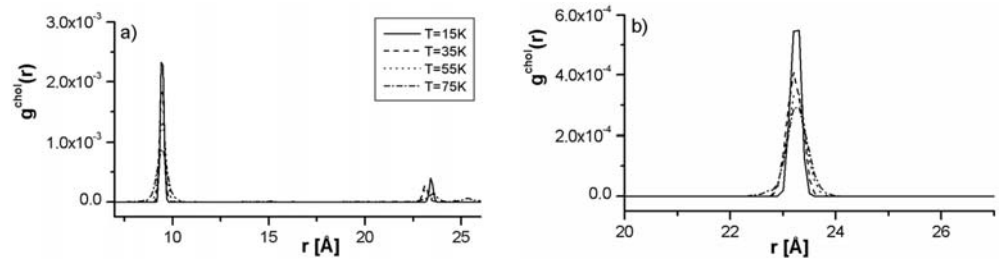

Fig. 12. The radial distribution function of the centre of mass of cholesterol for two concentrations and several temperatures: a) $SWNT(chol)_3(water)_{45}$ and b) $SWNT(chol)_2(water)_{80}$

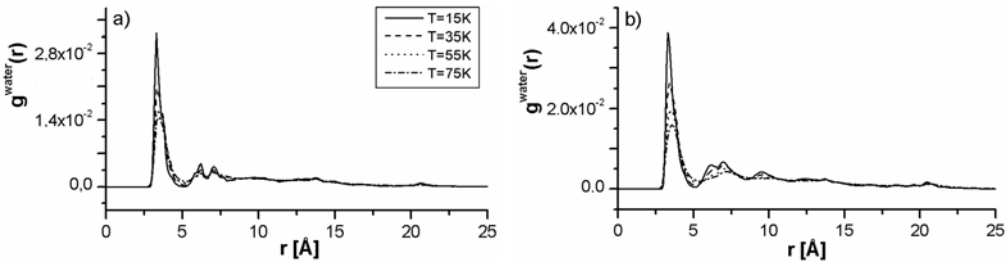

Fig. 13. The radial distribution function of the centre of mass of water for two concentrations and several temperatures: a) $SWNT(chol)_3(water)_{45}$ and b) $SWNT(chol)_2(water)_{80}$

The pronounced peak of $g_{chol}(r)$ at the large distance of $r \approx 23$ Å comes from two cholesterol molecules which happened to be positioned on the opposite side of the nanotube (for the snapshot of this configuration see Fig. 14).

The first peak of the $g_{water}(r)$ functions corresponds to the nearest neighbours average distance of water molecules surrounding the nanotube. As expected, the highest first peak corresponds to completely frozen water at $T = 15$ K and the lowest first

peak corresponds to the liquid phase at $T = 75$ K. The translational velocity autocorrelation functions for the cholesterol $C_{\vec{v}}^{\text{chol}}(t)$ and water $C_{\vec{v}}^{\text{water}}(t)$ molecule are given in Figs. 15 and 16, respectively.

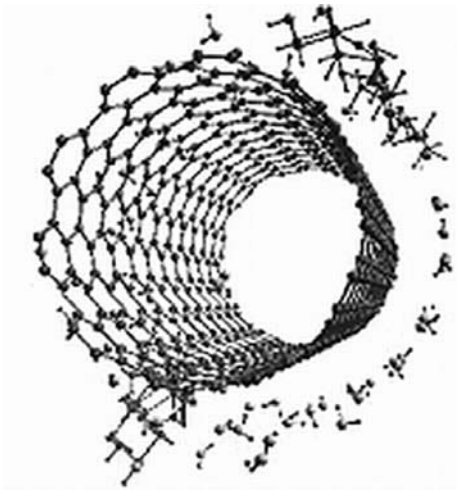

Fig. 14. Snapshot of the instantaneous configuration of SWNT(chol)$_2$(water)$_{80}$ at a temperature of $T = 55$ K

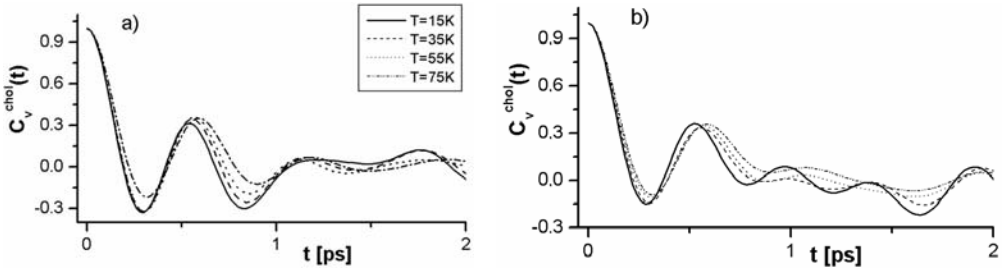

Fig. 15. The linear velocity autocorrelation function $C_{\vec{v}}^{\text{chol}}(t)$ of the centre of mass of the cholesterol molecule for two concentrations at several temperatures: a) SWNT(chol)$_3$(water)$_{45}$ and b) SWNT(chol)$_2$(water)$_{80}$

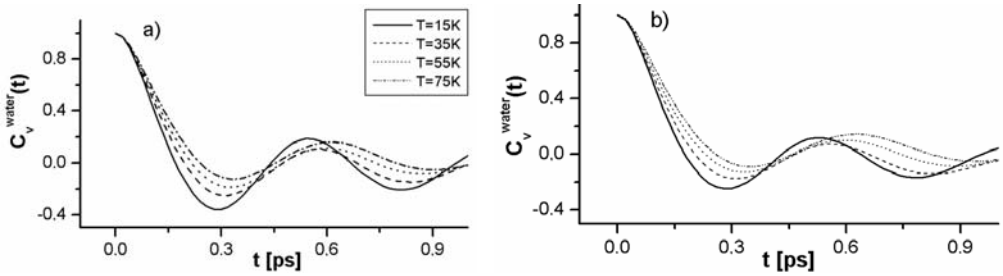

Fig. 16. The linear velocity autocorrelation function $C_{\vec{v}}^{\text{water}}(t)$ of the centre of mass of the water molecule for two concentrations at several temperatures: a) SWNT(chol)$_3$(water)$_{45}$ and b) SWNT(chol)$_2$(water)$_{80}$

One can see a slight temperature and concentration sensitivity of $C_{\vec{v}}^{\mathrm{chol}}(t)$ for such a large molecule as cholesterol. Contrary to this, the $C_{\vec{v}}^{\mathrm{water}}(t)$ of the light water molecule significantly depends on temperature. The dumped oscillations of $C_{\vec{v}}^{\mathrm{water}}(t)$ in the solid phase at low temperature (T = 15 K) becomes gradually smoother and featureless when the water is liquid (T = 75 K). The time scale of the decay of $C_{\vec{v}}^{\mathrm{chol}}(t)$ and $C_{\vec{v}}^{\mathrm{water}}(t)$ is quite different, which reflects the disproportion between masses of cholesterol and water. The representative examples of the Fourier transforms $FT(C_{\vec{v}}^{\mathrm{chol}}(t))$ and $FT(C_{\vec{v}}^{\mathrm{water}}(t))$ are presented in Figs. 17 and 18, where a distinct difference between $FT(C_{\vec{v}}^{\mathrm{water}}(t))$ of frozen and liquid water is clearly observed.

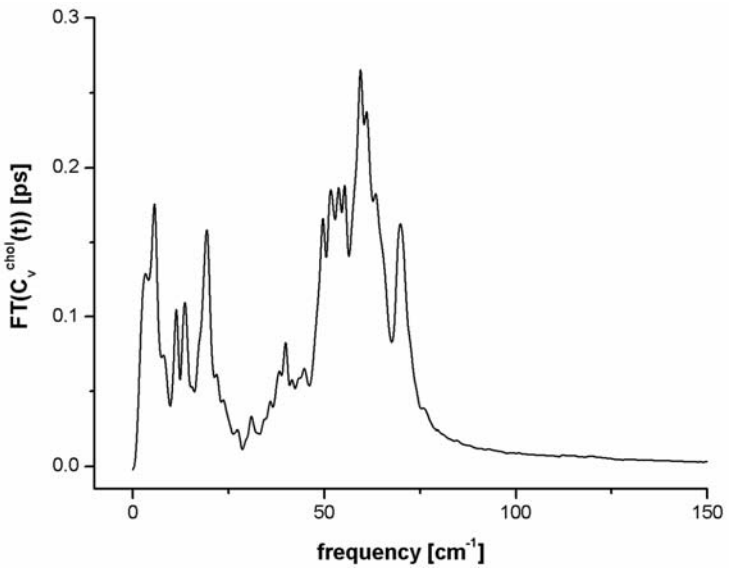

Fig. 17. An example of the Fourier transform $FT(C_{\vec{v}}^{\mathrm{chol}}(t))$ of the linear velocity correlation function of cholesterol for SWNT(chol)$_3$(water)$_{45}$ at T = 55K.

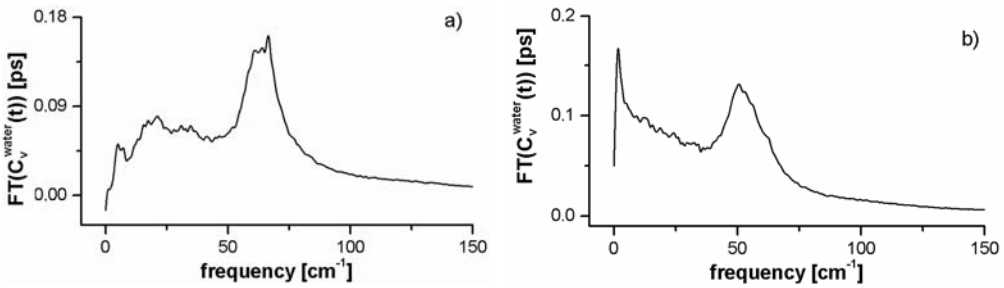

Fig. 18. An example of the Fourier transform $FT(C_{\vec{v}}^{\mathrm{water}}(t))$ of the linear velocity correlation function of the water molecule in solid a) and liquid b) phase of SWNT(chol)$_2$(water)$_{80}$

4. Conclusion

The preliminary MD simulations reported here may encourage future experimental studies, for example Raman spectroscopy, of carbon nanotubes coated by pure cholesterol and cholesterol–water mixture.

References

[1] IJIMA S., Nature, 354 (1991), 56.
[2] ODOM T. W., HUANG J.L., KIM P., LIEBER C.M., Nature, 391 (1998), 62.
[3] O'CONNEL M J., BACHILO S.M., HUFFMAN C.B., MOORE V.C., STRANO M.S., HAROZ E.H., RIALON K.L., BOUL P.J., NOON W.H., KITTRELL C., MA J., HAUGE R.H., WEISMAN R.B., SMALLEY R.E., Science, 297 (2002), 593.
[4] FAN S. WEI B.Q., VAJTAI R., JUNG Y., WARD J., ZHANG R., Science, 283 (1999), 512.
[5] KONG J. FRANKLIN N.R., ZHOU C., CHAPLINE M.G., PENG S., CHO K., DAI C., Science, 287 (2000), 622.
[6] ISLAM M.F. ALSAYED A.M., DOGIC Z., ZHANG J., LUBENSKY T.C., YODH A.G., Phys. Rev. Lett., 92 (2004), 088303-1.
[7] DRESSELHAUS M. S., DRESSELHAUS G. AND EKLUND P. C., *Science of Fullerenes and Carbon Nanotubes*, Academic Press, New York, 2000.
[8] DAWID A., GBURSKI Z., J. Phys. Condens. Matter, 15 (2003), 2399.
[9] ALLEN M.P., TILDESLEY D.J., *Computer Simulation of Liquids*, Oxford University Press, Oxford, 1989.
[10] DAWID A., GBURSKI Z., Phys. Rev. A, 68 (2003), 065202.
[11] JORGENSEM W.L., MADURA J. D., CHANDRASEKHAR J., J. Chem. Phys., 79 (1983), 926.
[12] SOKÓŁ M., DAWID A., DENDZIK Z., GBURSKI Z., J. Mol. Struct., 704 (2004), 341.
[13] RAPAPORT D.C., *The Art of Molecular Dynamics Simulation*, Cambridge University Press, Cambridge, 1995.
[14] KACZOR K., PAŁUCHA S. AND GBURSKI Z., J. Mol. Struct., 608 (2002), 9.

Received 6 September 2004
Revised 13 January 2005